Graduate School Form 30
Updated 1/15/2015

PURDUE UNIVERSITY
GRADUATE SCHOOL
Thesis/Dissertation Acceptance

This is to certify that the thesis/dissertation prepared

By Mayuresh P Bhasagare

Entitled

THREE-PHASE MULTILEVEL SOLAR INVERTER FOR MOTOR DRIVE SYSTEM

For the degree of Master of Science in Electrical and Computer Engineering

Is approved by the final examining committee:

Dr. Euzeli dos Santos
Chair

Dr. Brian King

Dr. Lingxi Li

To the best of my knowledge and as understood by the student in the Thesis/Dissertation Agreement, Publication Delay, and Certification Disclaimer (Graduate School Form 32), this thesis/dissertation adheres to the provisions of Purdue University's "Policy of Integrity in Research" and the use of copyright material.

Approved by Major Professor(s): Dr. Euzeli dos Santos

Approved by: Dr. Brian King 4/16/2015

Head of the Departmental Graduate Program Date

THREE-PHASE MULTILEVEL SOLAR INVERTER FOR MOTOR DRIVE SYSTEM

A Thesis

Submitted to the Faculty

of

Purdue University

by

Mayuresh P Bhasagare

In Partial Fulfillment of the

Requirements for the Degree

of

Master of Science in Electrical and Computer Engineering

May 2015

Purdue University

Indianapolis, Indiana

For the best parents and sister anyone could ask for:

Prasad, Sunanda and Priyanka Bhasagare.

ACKNOWLEDGMENTS

Many people have supported me throughout my career, but I can't even begin to imagine how lost I would have been without my parents. I dedicate this thesis to Dad and Mom, and also to my sister, who made me smile and took away all the pressure. Words will not be sufficient to describe the ways in which Ruta motivated me and always kept me going, thank you for being the true friend.

I would like to thank the ECE department at IUPUI for giving me the opportunity of studying and doing research with them. Dr. Euzeli dos Santos was unbelievably helpful, no matter what time of the day it was. He made things really simple with his awesome insights. I also am very grateful to Omar, without whom I would have needed a lot more time to finish my work, thank you for the nonstop help. I would also say a special thanks to Sherrie, for making sure I do not miss my deadlines, aiding me in editing my thesis and helping me whenever needed.

Lastly I would like to thank my relatives and friends for their continued support throughout my education.

TABLE OF CONTENTS

Page

LIST OF FIGURES

Figure Page

ABSTRACT

Bhasagare, Mayuresh P. M.S.E.C.E, Purdue University, May 2015. Three-Phase Multilevel Solar Inverter for Motor Drive System. Major Professor: Euzeli dos Santos Jr.

This thesis deals with three phase inverters and the different control strategies that can be associated with an inverter being used together. The first part of this thesis discusses the present research in the fields of PV panels, motor drive systems and three phase inverters along with their control. This control includes various strategies like MPPT, Volts-Hertz and modulation index compensation. Incorporating these techniques together is the goal of this thesis. A new topology for operating an open end motor drive system has also been discusses, where a boost converter and a flyback converter have been used in cascade to run a three phase motor. The main advantage of this is increasing the number of levels and improving the quality of the output voltage, not to mention a few other benefits of having the proposed circuit. A new algorithm has also been designed for starting and stopping the motor, which controls the current drawn from the power source during starting.

1. INTRODUCTION AND STATE OF THE ART

1.1 Introduction

Electric energy, being a big problem in many countries has become a wide subject for research, especially in finding various alternatives to non-renewable sources of energy. Solar energy is one such unlimited source of energy, which if tapped to its full potential will eliminate energy crisis in most places in the world. It has been the fastest growing source of energy in the past few years, especially in the field of electricity generation [3]. In the past 15 years, the demand of photovoltaic energy has increased by 25%, while the cost of PV has reduced by 4% [2],[3]. It is implied that this demand is going to increase in the future.

Photovoltaic panels consists of cells made up of semiconducting material. The photons absorbed by these cells from the solar energy exciting the electrons from their atoms, causing the flow of electrons, thus generating electricity. The electricity generated heavily depends on the amount of energy available at the solar cells. To maximise this energy, the panels need to be aligned in a particular direction. This direction can be known by checking the location and the local time of sunrise and sunset at a particular place. The direction is called as True south [4]. This will ensure that the panels are extracting maximum available energy during the day without having to change its orientation.

Owing to the growing implementation of photovoltaic energy, it is imperative that maximum energy is used out of it. This can be achieved with the help of power electronics. Photovoltaic cells will act as a source of DC voltage, which can be converted into various types of voltage using power electronic converters. Lower DC voltages can be converted to higher levels by the use of boost converter, flyback converters, buck-boost converters [7].

With the advent of more efficient power electronic inverter topologies like NPC and ANPC topologies [5], DC to three phase AC conversion has become simpler and more effective while the topologies talked about in [6] are proven methods for single phase AC to three phase AC conversion. While converting from DC to three phase AC, the quality of the AC waveforms depends a lot on the number of waveforms. A conventional three phase inverter is expected to give an output with lower levels while advanced and cascaded topologies are known to give multiple levels in the AC voltage thus reducing the harmonic distortion. These are talked about extensively in [8-13].

The goal of my research is to explore ways in which the available solar energy can be harnessed for daily purposes, especially in places which do not lie in close proximity to energy grids.

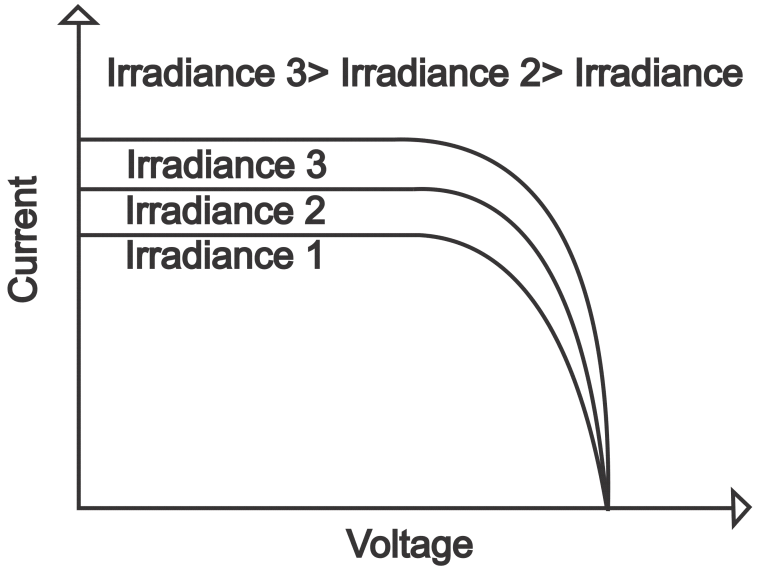

Fig. 1.1. I-V curve for a PV panel

The thesis talks about using solar energy to run a 3 phase motor. For this to be achieved, two things are of prime importance. Firstly, so as to operate the motor at maximum torque per ampere, its flux has to be kept at its rated value [1]. This will be

taken care of by Volts-Hertz method where the flux is kept constant by keeping voltage to frequency ratio constant. Irrespective of the input coming from the solar panels, when the input voltage is sufficient enough to run the motor at its rated conditions, the average value of the voltage applied to the motor should be maintained constant at its rated condition. This can be done by implementing the modulation index compensation method. In case of below rated and above rated condition operation, the above two methods are very essential in order to avoid overheating or premature stopping of motor. Secondly, a solar panel source has an I-V curve or a P-V curve, shown in Fig. 1.1 and Fig. 1.2. However, energy will not be used at its optimum rate if maximum power is not drawn from it. As a result, Maximum Power Point Tracking becomes equally important.

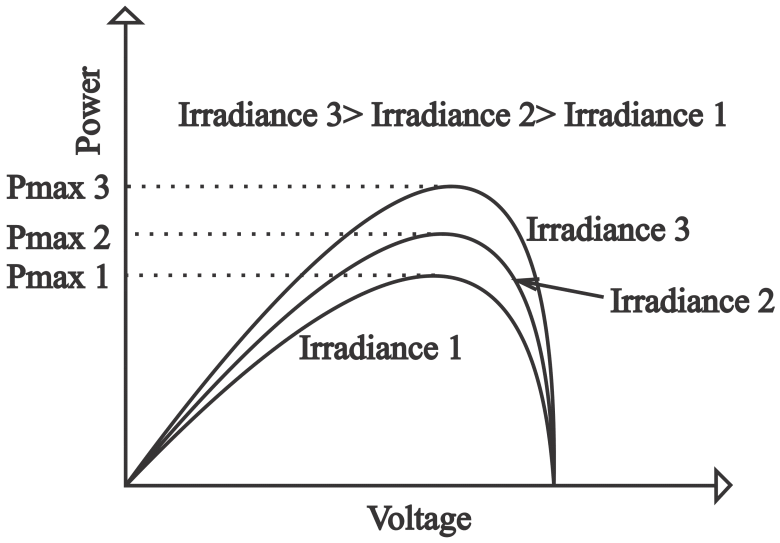

Fig. 1.2. P-V curve for a PV panel

In order to obtain sufficient voltage, 6 solar panels of 140 W are needed. These 6 solar panels can be connected in series, 2 of them dedicated to nourishing a part of their energy to power up the microcontroller and power electronic devices. Thus the remaining energy from these 2 panels and the output of the other 4 panels will

act as the usable source for power conversion. Because of the series connection, the total input voltage will be the sum of the voltages of the panels, while the current will remain constant.

This thesis has been organised in the following manner. The latter part of this chapter deals with the state of the art. Chapter 2 deals with the implementation methods. They are MPPT and Volts-Hertz method. The third chapter discusses a multilevel solar inverter for an open end winding motor drive system which will explain a new multilevel topology for a motor. Fourth chapter enlists the hardware setup implementing a 3 phase solar inverter with MPPT, Volts-Hertz and modulation index compensation techniques. In the next chapter, the hardware and simulation results can be seen, with the last chapter throwing light on the conclusion of the experimental and simulation results.

1.2 State of the Art

1.2.1 Control Strategies for PV

A lot of research has been already done on control strategies for PV panels. Fig. 3 shows the classification with a few of the most commonly used strategies. PV panels are essentially current sources being controlled according to the design [16]. The data in [14] talks about nonlinear control strategy for PV generator systems for controlling the grid frequency and voltage. It gives a good solution for frequency control using the DC-DC boost converter and voltage control in DC-AC converter. In [15], there is an extensive description for voltage and frequency regulation combined with MPPT. In order to control all these parameters in the system, a controller needs to be present [17-23]. This can be either a microcontroller or any supervisory control system.

Being an irregular source of energy, it can be unreliable at times. However strategies have been generated to compensate for this disadvantage. This includes using batteries to make up for a lower voltage [24-28] and charging these batteries when no load is connected across the system. These batteries can also be used as substitutes

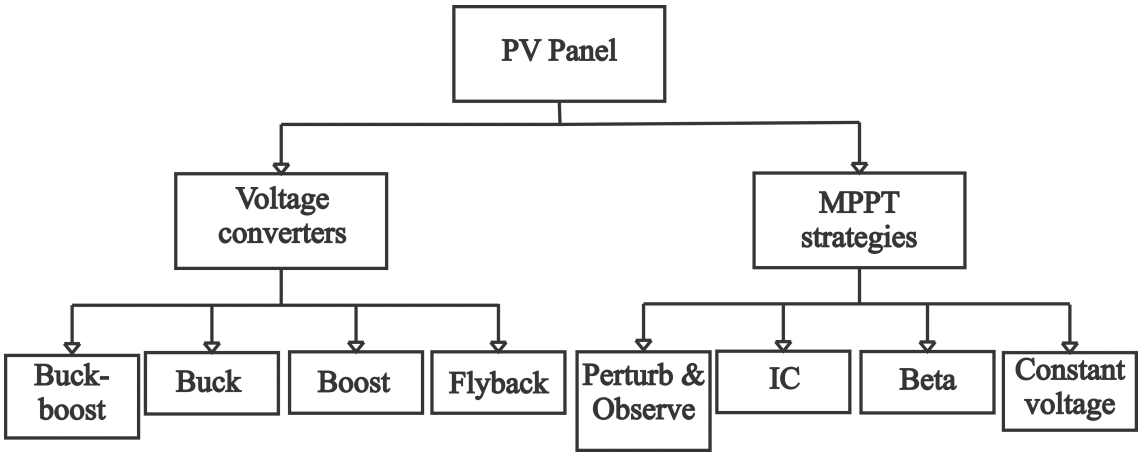

Fig. 1.3. Control of PV Panels

when there are grid interruptions [29-30]. Even with these batteries, control has been designed so as to achieve MPPT when charging with PV panels. [31] describes how that is achieved with the help of Perturb and Observe method for MPPT, which controls the duty cycle for the DC to DC converter. Maximum power point tracking (MPPT) is also an important tracking technique required to extract maximum possible power from the PV panel. Various strategies like Beta method, IC method, Perturb and Observe method have been explored [33] and studies have proved that Beta method is the best method when it comes to power point tracking [32]. Grid connection for Solar inverters has been regarded highly in the field of research, even a half bridge converter can be used for that [68].

As seen above, extensive research has been done in control and a mixture of these techniques have been implemented in this thesis.

1.2.2 Three-Phase Motor Drive System

Three phase motors have had numerous applications in various fields. Being robust, they have been apt for use in industries. Subsequently, a lot of research has been done to improve the efficiency of the motors and there have been a lot of tweaks

in designs to suit the motor for a particular application. Motors have been designed for high speed, low speed, medium speed and even variable speed applications.

A few vehicles use power grids to charge their batteries. But means have been found to use a motor to charge the batteries in traction application [34]. It states how 3 phase motors can be used for operation in multiple modes, one where it operates as a 3 phase motor and the other mode where it acts as an isolating transformer which gives 3 phase voltage to the inverter to charge batteries. Variable speed 3 phase motors have been used for traction applications in various kinds, that is, as a 3 phase motor and even as a single phase motor as described in [35]. Motor drive system configuration to be used in an electric vehicle to drive the vehicle and their lifetime reliability has been talked about in [36]. One third of the electrical energy consumption being residential consumers, motors are involved in residential applications as well. Motor drive systems are known to be used in residences for washing machines and other similar applications [37] efficiently, while reducing cost of production by using a buck-boost technique to control the output voltage and also reducing the complexity of the circuit simultaneously.

Since this thesis talks about PV energy being harnessed for motor use, its primary need will be in farming in areas where electricity is not easily available. The main application there will be pumps. Research has been done on this application as well. [38] talks about the use of PV cells to run a Switch Reluctance Motor for pump applications. It describes this application in different modes where the motor can run and even a battery can be charged in different modes. A cascaded configuration can also be used in the inverter for a better quality 3 phase voltage [39], along with the application of MPPT and Volts-Hertz control incorporated.

1.2.3 Three Phase Inverter

With the advent of power electronic devices, a lot of new configurations have been designed for power conversion, be it DC to DC or AC to AC or AC to DC or DC to

AC. Three phase inverters have been widely used DC to 3 phase AC conversions. A lot of topologies have been developed only in the area of inverters. A three phase load can be supplied by 3 separate H-bridge inverters [41]. PWM strategy for that will differ and another disadvantage of this is that more number of switches will be needed. A conventional 3 phase inverter can be used along with other DC to DC converters successfully [40], thus using different control strategies together. A coupled inductor inverter [45] gives a very high level 3 phase output, thus improving the quality of the waveform.

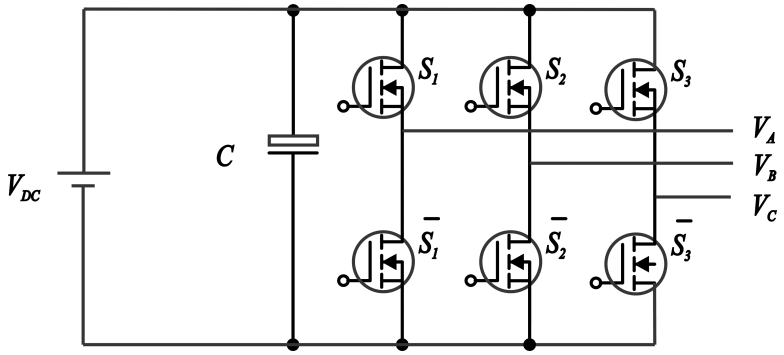

Fig. 1.4. A conventional Three-Phase Inverter

Waveform quality can also be improved by using cascaded configurations [42-43]. The number of levels can be increased by adding more inverters, which is in cascaded connection. In case of a motor application, an open winding motor can be used so as to use 2 inverters with their pole voltages appearing across the 6 ends of the windings [44]. Chapter 3 discusses this in detail.

2. VOLTS - HERTZ AND MPPT CONTROL STRATEGIES

2.1 Volts - Hertz Method

The Volts-Hertz method is essentially used for variable frequency drives where the voltage and frequency are adjusted so as to run the motor efficiently with the rated flux [46], [47]. This ensures maximum torque per ampere [1]. It was the first method in the history of inductions motors to operate them without losses [54]. Its major application has been in variable frequency drives, the motor has to run at different frequencies at different points of operation. Increasing quality of solid state inverters has only caused this method to be used widely in variable speed drives [55-57]. Research done in [53] shows how Volts-Hertz method can be used to ensure high output torque and close to zero steady state speed error for low speed applications at any frequency.

However, here it is not used for the same purpose. The voltage available from the PV panel at times may not be sufficient to run the motor at its rated value. To guarantee that the motor is being operated at its maximum possible torque for that particular current, Volts-Hertz comes handy.

In this implementation, when the motor is being operated at voltages lower than its rated value, an equation has been used to define the frequency of the reference voltages of the PWM signals applied to the inverter. The rated values of the motor being used are 60 Hz and 120Vrms or approximately 170 V peak. When operating the motor below 120Vrms, the frequency needs to be adjusted accordingly. Thus when the motor is operating at 60Vrms, the frequency should be kept constant at 30 Hz, so the ratio remains constant as in equation 2.1.

$$\frac{V_{rated}}{F_{rated}} = \frac{170}{60} = 2.83 \tag{2.1}$$

2.1.1 Implementation

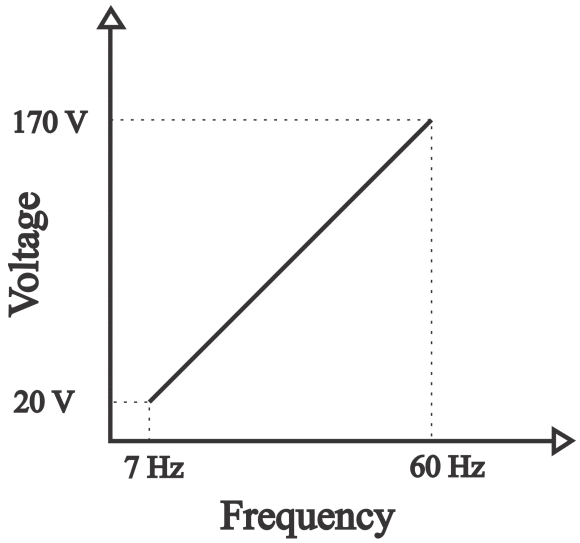

Fig. 2.1. Volts - Hertz strategy

Fig. 2.1 shows the references for frequency being used for the operation of the motor at voltage values lower than its rated condition. This operation should take place only when the voltage is between 20V and 170V. If the voltage applied to the motor is below 20 V, the motor should not run. The DC link voltage of the inverter is sensed and sent to the dsPIC33FJ64MC802 in order to define the frequency for PWM signals in the low voltage operation. Since the dsPIC can only sense voltages upto 3.3V, the DC link voltage needs to be scaled from the higher value to a smaller one. Assuming that the DC link voltage can reach a maximum of 350 V, with the design of the panels and duty cycle of the boost converter via MPPT, voltage dividers were designed to scale that voltage down to 3.3 V using the formula in equation 2.2.

$$V_{dcread} = V_{dc}\frac{R_2}{R_1 + R_2} \tag{2.2}$$

The voltage sensed by the dsPIC is scaled to another value. It appears to convert the read values into numbers between 0 and 1023. The maximum value read by

the dsPIC, 3.3 V, is interpreted as 1023, while 0 V is read as 0. This relationship is linear. Thus, another equation is needed to convert the read value to the actual voltage arriving at the particular pin of the dsPIC and then rescaling it to the DC link voltage using the reverse of the above equation. All these conversions of voltages have been done in code for the dsPIC.

Knowing the rated value of the motor as 120Vrms and its rated frequency as 60Hz, we know that the ratio of V/f has to be 3.4. Thus the voltage read will define the frequency of the reference voltage used for PWM as shown in equation 2.3-2.5.

$$F = \frac{V_{dcread}}{2.83} \tag{2.3}$$

$$theta = theta + 2\pi Fh \tag{2.4}$$

In equation 2.4, h is the step size and $theta$ is the angle defining the sinusoidal waveform.

$$V_{aref} = \frac{V_{dc} m_a sin(theta)}{2} \tag{2.5}$$

Similarly, the reference voltages can be defined for the PWM of the other 2 phases. Thus this implementation makes sure that the voltage to frequency ratio remains constant, maintaining the flux at its rated value.

2.2 MPPT

In order to extract maximum energy from the PV panel, there has to be a certainty of operating the panel at maximum possible power. There are various techniques which can be used to implement MPPT[48-51]. Some of the being PO method, CV method, IC method and Beta method. Even though the analysis in [49] infers that the Beta method is the most efficient, it needs to know the exact electrical parameters of the PV panel, which does not allow it to be generalised for any panel. As a result, the PO method is being preferred here since it does not require any knowledge about the parameters of the panel.

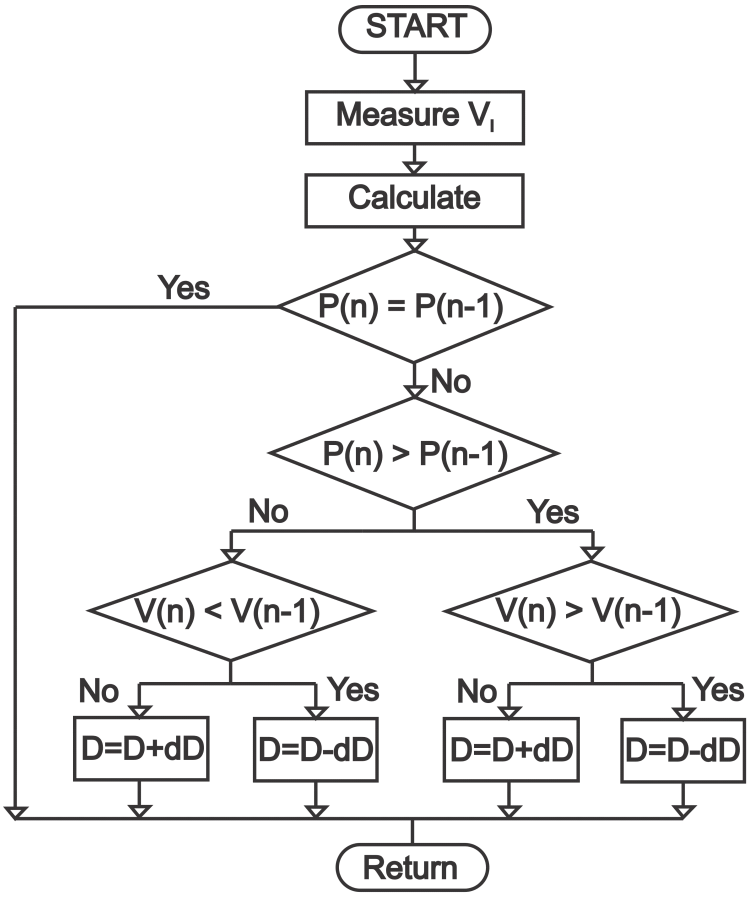

Fig. 2.2. Perturb and Observe algorithm

The PO method needs the knowledge of the current and the voltage coming from the panel. This method basically ensures Maximum power point operation by constantly comparing the present value of power with the previous value and adjusting the voltage extracted from the PV panel. Thus, if the power is increasing, the change in voltage should continue until the power measures becomes lesser than its previous value. Thus there will be a change in the direction of voltage variation, which will again increase power. The Fig. 2.2 shows the algorithm used for perturb and observe method.

2.2.1 Implementation

The algorithm in Fig. 2.2 was converted into a C code and programmed on the dsPIC33FJ64MC802 with current and voltage being sensed by the dsPIC with the help of a current sensor and a voltage regulator being present on the circuit. This implementation ensures that the panel is operating at its maximum power rating at all times, irrespective of the type or rating of the PV panel which was a problem in some of the other MPPT methods [49].

Just like in Volts-Hertz, the input voltage level would be too high for the dsPIC and as a result it will have to be converted to a smaller value with the maximum achievable voltage from the solar being converted to 3.3V for the dsPIC to be read. For this, another voltage divider was used. Since the maximum possible voltage available from 6 panels is 126 V, a voltage divider was designed to convert 126 V to 3.3 V.

A current sensor has been used to sense the value of the current. The current sensor used is capable of sensing currents up to 10 A. If the current flowing through it is 0A, the output of the current sensor would be 1.5 V. As current increases, the output voltage of the current sensor reduces from 1.5 V with a scale of 0.132V/A.

Since these voltage levels are very small, a first order low pass filter was used so as to eliminate the high frequency components created by noise or EMI in the circuit. Perturb and Observe method was implemented using the algorithm in Fig. 2.2 to guarantee Maximum Power Point Tracking.

3. THREE-PHASE SOLAR INVERTER FOR OPEN-END MOTOR DRIVE SYSTEM

3.1 Introduction

Among the many applications of photovoltaic energy, pumping is one of the most promising especially in either rural or remote areas where the electrical grid is not available [58]. In a photovoltaic pump-storage system, solar energy is stored, when sunlight is available, as potential energy in a water reservoir and consumed according to demand.

Most of the power electronics configurations employed in a three-phase induction motor-pump system is constituted by a DC-DC converter at the first stage while a DC-AC inverter is used to feed the induction motor [59]. The maximum power point tracker (MPPT) is of the solar panels is guaranteed by the DC-DC converter [60-61].

Different topologies have been explored in the technical literature to implement the DC-AC converter in photovoltaic applications, which includes multilevel converters cite three papers of multilevel converters applied in PV systems. Among the multilevel topologies, the open-end-winding (OEW) converters has some advantages in comparison with other multilevel topologies, such as: i) power switches with lower voltage level, ii) reduced harmonic distortion and iii) reduced converter losses.

This chapter proposes the topology presented in Fig. 3.1, which is constituted of two three-phase inverters series connected to an open-end motor drive system. Each inverter is connected to a set of solar panels through dc-dc converters. While the Inverter 1 is connected to a non-isolated conventional boost converter, Inverter 2 is attached to an isolated fly-back topology.

The fly-back converter eliminates any circulating current and brings the benefit of having a voltage v_{C2} independent of v_{C1}, which will be explored to increase the

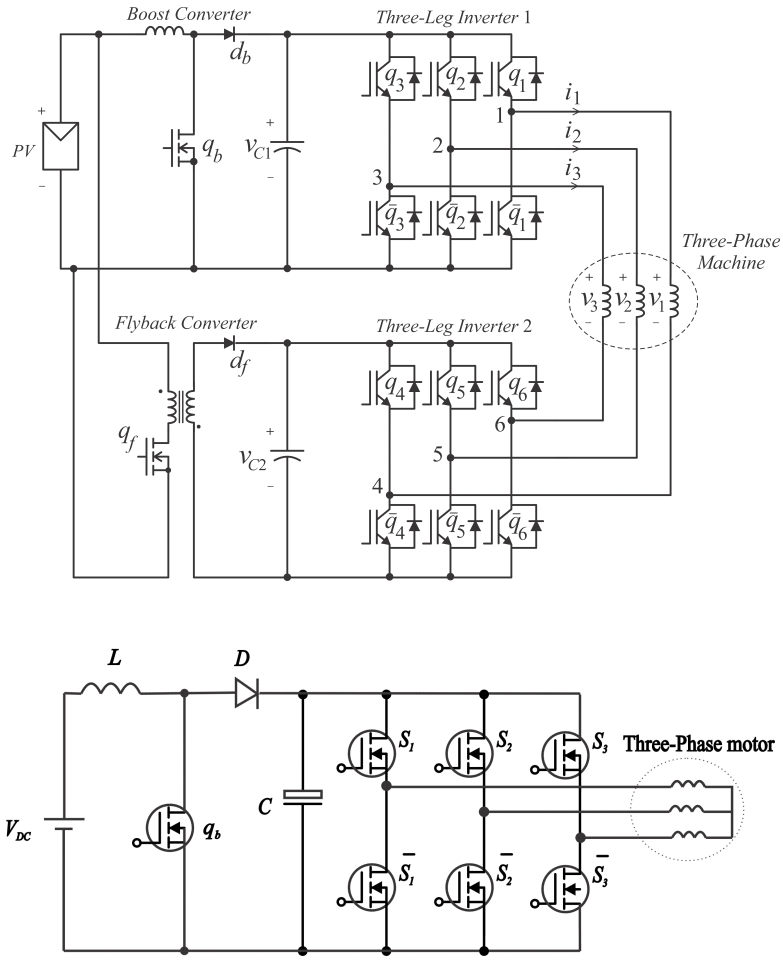

Fig. 3.1. (a) Proposed motor drive system. (b) Conventional three-phase motor drive system.

number of levels applied to each phase of the motor. The main advantages of the proposed configuration as compared to the conventional one in Fig. 3.1(b) are: 1) better quality of the motor phase voltage; 2) dc-dc converter operating with conversion ratio, which reduces the stress over the power switch; and 3) lower dc-link capacitor losses.

3.2 DC-DC Conversion Units

The function of both boost and fly-back converters on the proposed topology [see Fig. 3.1(a)] is to guarantee maximum power point operation with a P and O MPPT strategy [64] as well as to increase the number of levels of the voltage applied to the motor [63].

The boost converter is chosen to implement the MPPT while the fly-back topology feeds Inverter 2 with double of the voltage of Inverter 1. Although the roles of both converters could be switched, the implementation as described previously increases the efficiency of the dc-dc conversion stages by avoiding high duty cycle operations. Notice that the input-output voltage ratio for the boost and fly-back converters are given respectively by:

$$\frac{v_{C1}}{V_{PV}} = \frac{1}{1 - D_b} \tag{3.1}$$

$$\frac{v_{C2}}{V_{PV}} = N\frac{D_f}{1 - D_f} \tag{3.2}$$

where D_b, D_f and N are the duty cycle of the boost converter, duty cycle of the fly-back converter and the high-frequency transformer ratio, respectively.

3.3 Open-end Motor drive system

The conduction state of all power switches will be represented by homonymous binary variables and q_1, q_2, q_3, q_4, q_5, and q_6, where $q_j = 1$ indicates a closed switch while $q_j = 0$ means open switch with j=1,2,3 and 4. The pair of switches $q_j - \bar{q}_j$ is complementary, i.e., $\bar{q}_j = 1 - q_j$. Notice that the pole voltages can be written as a function of the state of the switches, as following for the inverters 1 and 2, respectively:

$$v_{10_1} = (2q_1 - 1)\frac{v_{c1}}{2} \tag{3.3}$$

$$v_{20_1} = (2q_2 - 1)\frac{v_{c1}}{2} \tag{3.4}$$

$$v_{30_1} = (2q_3 - 1)\frac{v_{c1}}{2} \tag{3.5}$$

$$v_{40_2} = (2q_4 - 1)\frac{v_{c2}}{2} \tag{3.6}$$

$$v_{50_2} = (2q_5 - 1)\frac{v_{c2}}{2} \tag{3.7}$$

$$v_{60_2} = (2q_6 - 1)\frac{v_{c2}}{2} \tag{3.8}$$

A model of the open-end motor drive system presented in Fig. 3.1(a) can be obtained in term of pole voltages as following:

$$v_1 = v_{10_1} - v_{40_2} - v_{0_{21}} \tag{3.9}$$

$$v_2 = v_{20_1} - v_{50_2} - v_{0_{21}} \tag{3.10}$$

$$v_3 = v_{30_1} - v_{60_2} - v_{0_{21}} \tag{3.11}$$

Assuming a balanced case with $v_1 + v_2 + v_3 = 0$ and $i_1 + i_2 + i_3 = 0$, the voltage v_{0_21} is giving by:

$$v_{0_{21}} = \frac{1}{3}\sum_{i=1}^{3} v_{i0_1} - \frac{1}{3}\sum_{j=4}^{6} v_{j0_2} \tag{3.12}$$

3.4 Control Strategy

Fig. 3.2 shows the block diagram for the control strategy applied to the proposed configuration. The MPPT strategy is a Perturb Observe scheme as done in [62]. While the voltage (V_{PV}) and current (I_{PV}) are the inputs of the MPPT block, its output is the boost duty cycle (D_b). Notice that the voltage v_{C1}, the output voltage of the boost, will be a function of D_b. To guarantee a higher number of levels applied to the phases of the three-phase machine the fly-back topology will be controlled to assure that $v_{C2} = v_{C1}$. Also, the fly-back converter isolates the machine terminals 123 from 456, which eliminates any circulating current due to the open-end arrangement. Since the input voltage of both inverters (v_{C1} and v_{C2}) are a function of the MPPT, the control of the three-phase induction machine is implemented with the Volts/Hertz strategy to assure rated flux. The output of the Volts-Hertz/m_a compensation block

will define the reference voltages applied to the PWM block. The two inverters will generate a high quality output voltage.

If the DC link voltages are sufficient to run the motor at its rated value or more than that, then the modulation index compensation strategy comes into picture. The RMS value of the voltage across the phase of the motor depends upon the modulation index of PWM carriers. At modulation index 1, the RMS value of voltage across the phase of the motor will be at its maximum for those particular DC link voltages. If the modulation index is reduced, the RMS voltage across the phase reduces. This concept can be used to restrict the voltage across the phase at its rated value in the operating conditions wherein the input voltage has the capability of operating the motor at voltage values higher than its rated conditions. While Volts-Hertz strategy is being used for below rated conditions, the frequency of the motor operation is below its rated value as well. When the motor is running in the modulation index compensation mode, the frequency however, will be kept constant at its rated value.

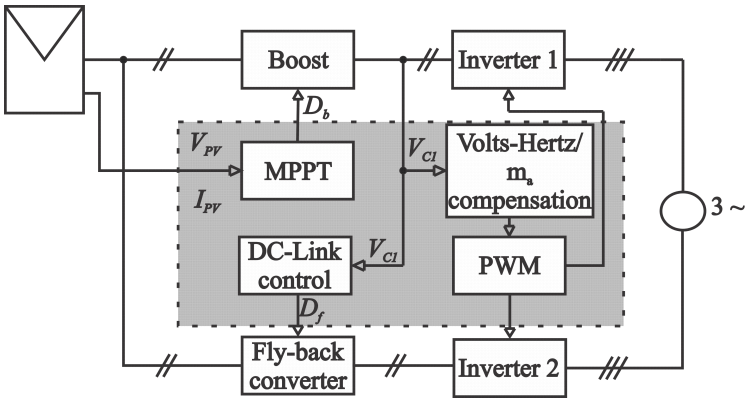

Fig. 3.2. Control scheme block diagram

3.5 PWM Strategy

The PWM strategy used for controlling the switches of the inverter hugely influences the quality of output voltage across the load. Harmonics can be reduced by

cascading the inverter configurations and also differing the voltage applied through these inverters to the load [66]. A variety of PWM strategies have been studied for different topologies for inverters in [65-66].

This application will use two different triangular waves with level shift strategy as illustrated in Fig. 3.3.

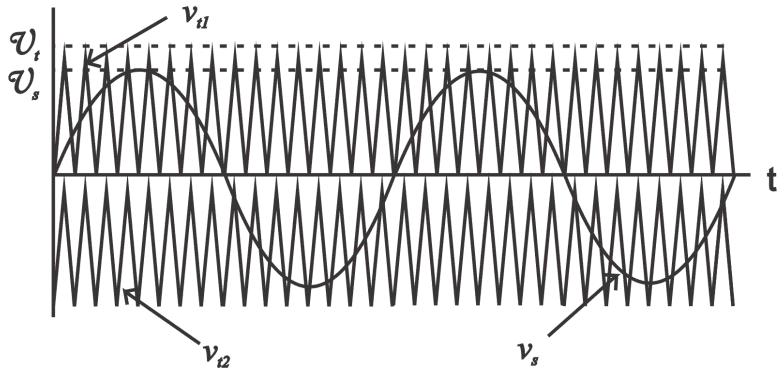

Fig. 3.3. PWM Strategy

V_{t1} and V_s define the PWM signals for Inverter 1, specifically for switch q_1. V_{t2} and V_s define the PWM signals for the Inverter 2, particularly $\bar{q}_6$. PWM signals for the switches in the other phases by simply phase shifting the sinusoidal wave by 120 degrees.

3.6 Start-up and stopping procedure

The starting current of an induction motor can reach as high as 6 to 7 times the rated value of the motor. Different methods or starting an induction motor are discussed in [67], along with their problems. In order to reduce the starting current of the motor here, the modulation index increment method can be used. As the modulation index directly controls the output voltage of the inverter, if it is increased gradually, the voltages across the phases of the motor will be increasing in a similar proportional manner, thus guarantying soft starting.

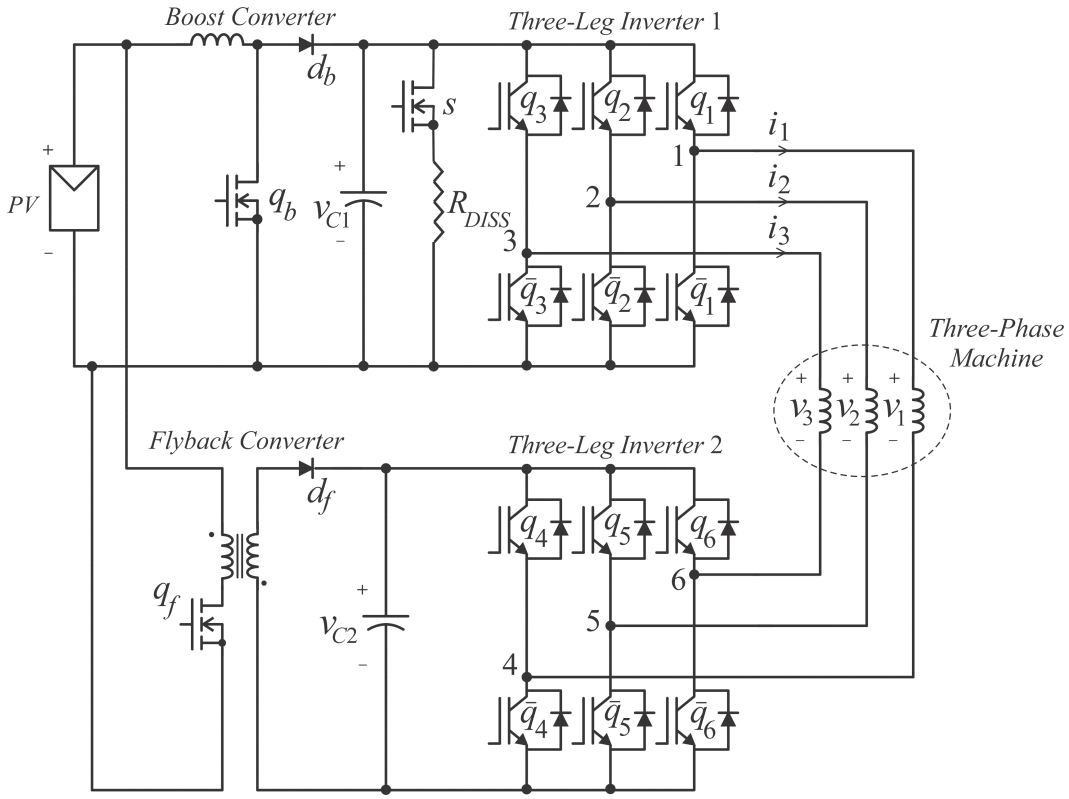

Fig. 3.4. Proposed circuit with starting and stopping control

Control of the motor can come from a separate switch altogether. The proposed algorithm uses this switch to choose the mode of operation. A very high value resistance along with a switch in parallel with the DC link capacitor is also needed so as to restrict the current to a low value when the external switch for motor is OFF. As a result, when the motor control switch for motor is OFF, the top switches of the inverter can be turned off, thus isolating the motor from the circuit. The resistance switch will the turned ON, making the resistor act as the load, keeping the current drawn from the panel small, which otherwise would be open circuited. If the switch were to be turned ON without that resistance, it would draw a huge current from the PV panels, thus shooting up the voltage of the boost inductors due to the high starting current requirement. Having the resistance in the circuit avoids that sudden huge current extraction from the panel.

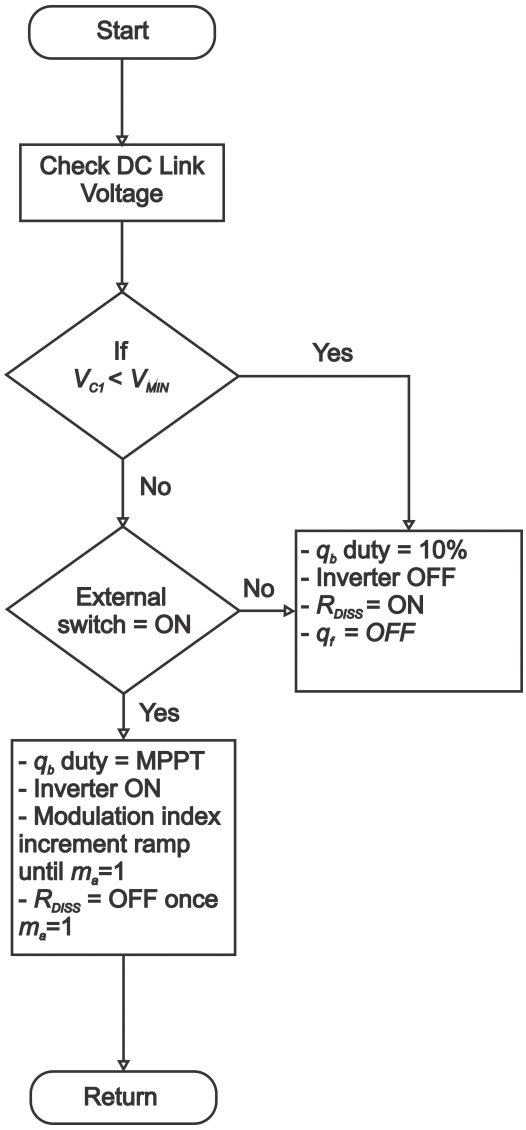

Fig. 3.5. Start-up procedure

Now in order to control the starting current of the motor, the voltage applied to the motor can be gradually increased by increasing the modulation index for the PWM applied to the inverter. This can act as a soft starter with the control of modulation. While the modulation index is being increased from 0.1 to 1, the resistance will still be connected in the circuit until modulation index becomes 1. This ensures low current in the circuit during the starting of the motor. Once modulation index

becomes 1, the motor will be the only load connected to the PV panel since the switch in series with the dissipation resistance will be turned OFF.

A similar strategy can be used to stopping the motor. When the motor switch is turned OFF, the same procedure can be followed in the reverse order, thus turning ON the dissipating resistance while the motor is still connected in the circuit with the modulation index reducing from 1 to 0. What this does is there is no sudden drop in the current in the circuit. Once the modulation index becomes 0, all the top inverter switches can be turned ON, making the lower switches OFF, thus disconnecting the motor from the circuit.

Also, there needs to be a lower limit of voltage for the operation of the motor. Below that lower limit voltage across the DC link capacitor, the PWM for the motor wont turn ON even if the switch for motor is ON. The modes of operation of this circuit can be seen explicitly in Fig. 3.6.

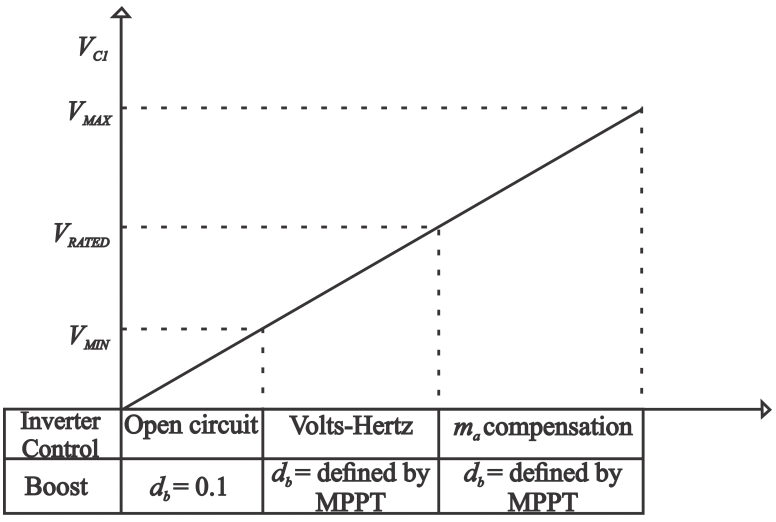

Fig. 3.6. Modes of operation of circuit based on voltage level

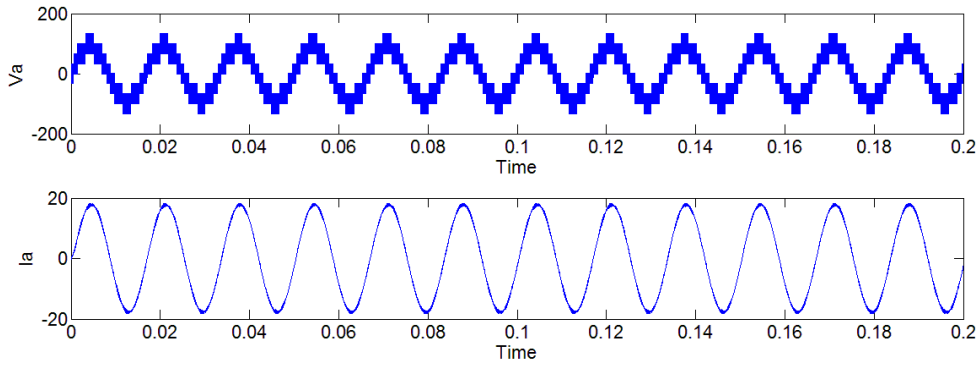

Fig. 3.7. Output voltage and current for proposed circuit

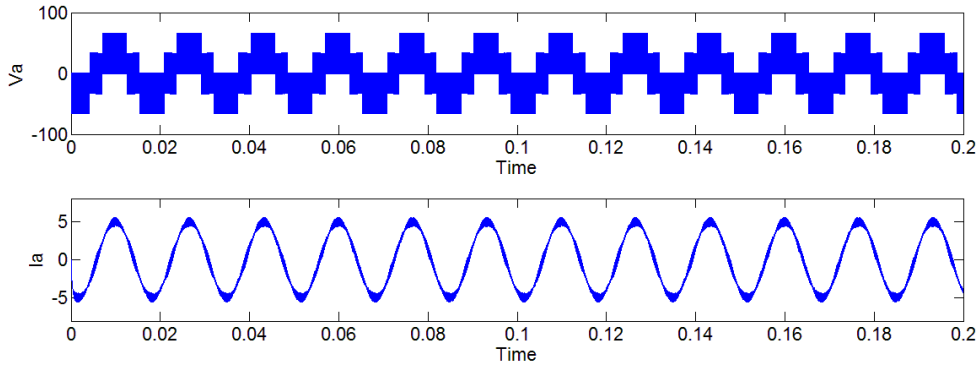

Fig. 3.8. Output voltage and current for conventional inverter

3.7 Comparison between conventional and proposed system

The number of levels of voltage obtained from the proposed system is 10, twice as much as the number of levels obtained from the conventional configuration. It is clearly observed that the quality of the waveforms has increased and is much closer to a sinusoidal wave. In technical terms, the THD for these voltages was obtained from the PSIM, the THD being 69% for the conventional configuration voltage, while it is 39% for the proposed configuration. This THD can be further reduced by the use of advanced PWM techniques.

The difference is also in the amplitude of the voltages. The voltage in Fig. 3.7 has an amplitude of 133 V, when v_{c1} and v_{c2} are 100 V. This can also be analysed using equations 9, 10 and 11. However in Fig. 3.8, the amplitude is 66.66 V when the DC link voltage is 100 V.

4. EXPERIMENTAL SETUP

4.1 Introduction

The proposed circuit in chapter 3 is the new strategy for motor operation with its windings open winded. The hardware setup was designed to test the conventional three phase solar inverter to run a three phase motor incorporating MPPT, Volts-Hertz, modulation index compensation and the start-up and stopping procedure in the same circuit.

The set this hardware up, a set of power electronic designs were used. A total of 6 panels were used to draw power from. Now in order to guarantee maximum power being extracted from the PV panels, MPPT needs to be implemented. It was done using the Perturb and Observe method, which defines the duty cycle of DC-DC converter. The DC-DC converter used was the boost converter. The output of the boost converter acts as the DC link voltage for the 3 phase voltage source inverter. To control all these processes, a dsPIC33F64MC802 was used. It was programmed using MPLab software in C language. A set of voltage regulators was used to convert a higher voltage level to a lower one in order to power up the devices which needed energy to run. A schematic of the circuit can be seen in Fig. 4.1.

4.2 Photovoltaic Panels

As mentioned previously, 6 photovoltaic panels were used, connected in series. Each panel used was 140 W, with rated voltage and current as 21 V and 7 A. More can be added in places where irradiance is lower. Due to the series connection, the total input voltage from the panel goes up to 126 V. Since a few devices in the setup

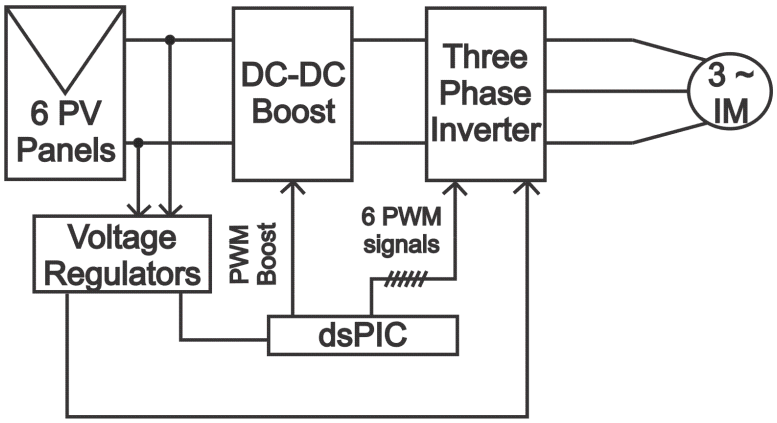

Fig. 4.1. Schematic of the hardware setup

like the dsPIC, Inverter and drivers need a power supply, lower voltage is needed. For this very reason, voltage regulators are being used. The inverter and drivers require 15 V supply, while the dsPIC needs 3.3 V. This voltage is provided by using 3 voltage regulators LM7824, LM 7815 and LM317.

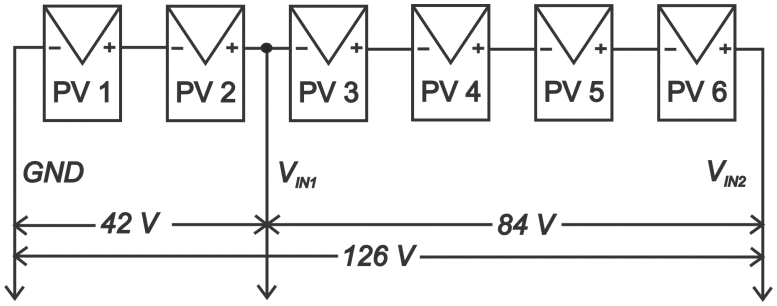

Fig. 4.2. Panel connection

To arrange for this lower voltage, there is an additional voltage coming from the PV panels as shown in Fig. 4.2. The positive of PV 2 has 2 connections, one going to the negative of PV 3 and the other going to the input LM7824 regulator. LM7824 has the capability of converting voltage to 24 V. The output of LM7824 is given to the input of LM7815, which returns a 15 V signal. This is sent to the inverter and drivers. It also goes to the input of LM 317, which is designed to give the output

as 3.2 V. This voltage is sent as an input to the dsPIC. It is also the supply for the current sensor.

Thus, V_{IN1} is the input for voltage regulators and V_{IN2} is the input voltage applied to the DC-DC Boost converter.

4.3 DC-DC Boost converter

DC-DC Boost converter in this circuit has been used for two purposes. Firstly to ensure that the panel is operated at its maximum power. The Perturb and Observe method for MPPT defines the duty cycle for the switch in the boost converter. Its second purpose is to boost the voltage to a higher value. A typical boost converter circuit is as in Fig. 4.3.

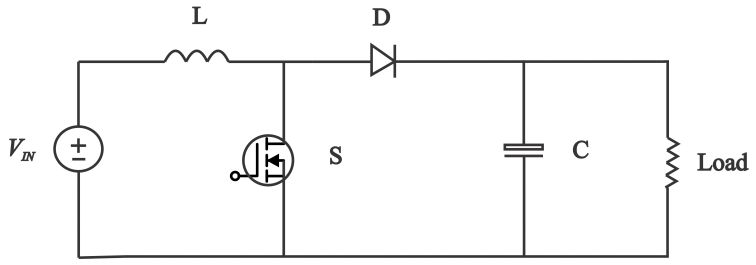

Fig. 4.3. Boost converter

This circuit boosts the input DC voltage to a higher value depending on the duty cycle of the switch S. In this implementation, a MosFET is preferred to be used as the switch due to their high switching speed capability.

The operation of this converter can be explained by Fig. 4.4 and Fig. 4.5. In Fig. 4.4, when the switch is closed, the inductor starts storing energy and the capacitor discharges to supply energy to the load. In Fig. 4.5, when the switch is open, the charged inductor releases its energy and adds to the energy from the input, which in turn charges the capacitor and supplies sufficient voltage.

The switch closes again to charge the inductor, this is a continuous fast process which results in the capacitor always staying charged at a value higher than the input

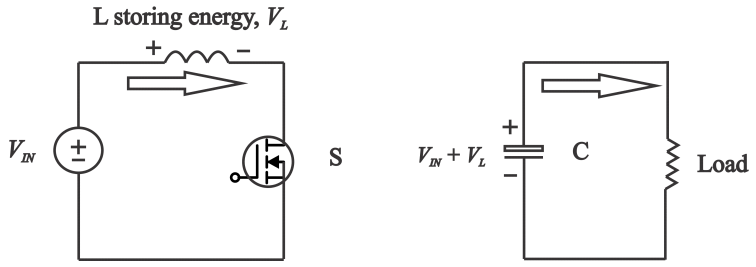

Fig. 4.4. Boost converter switch ON

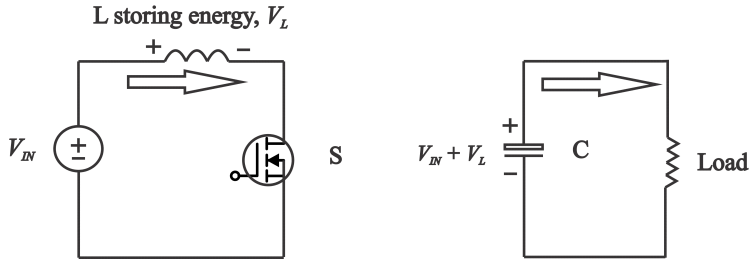

Fig. 4.5. Boost converter switch ON

voltage. This output voltage heavily on the duty cycle of the switch. The higher the duty cycle, the higher will be the output voltage. Equation 4.1 gives the equation for boost.

$$V_0 = \frac{V_{IN}}{1 - D_b} \tag{4.1}$$

4.4 Three-Phase Inverter

A conventional three phase inverter has been used in this hardware implementation. The PWM signals sent to the inverter give a five level phase to ground output or a three level phase to phase voltage. Instead of using six switches as shown in Fig. 4.6, a power electronic device named IRAMX20UP60A which acts like a conventional three phase inverter. It has a capability of handling 600V and 20 A. A 15 V voltage supply is required to turn it ON. This supply is obtained from LM7815. The PWM signals sent to the inverter come from the dsPIC.

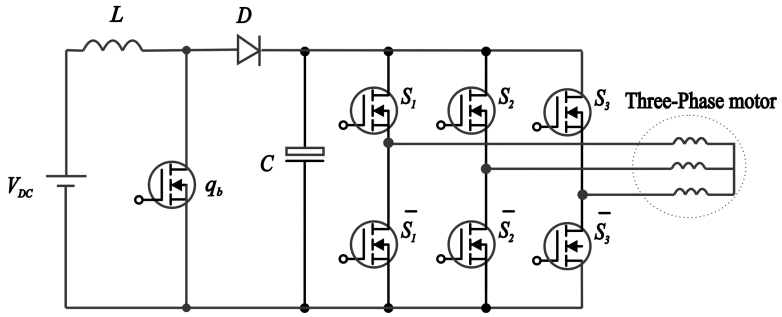

Fig. 4.6. Conventional three-phase nverter

4.5 dsPIC controller and associated drivers

A lot of different processes need to be controlled at the same time. These processes range from computing the duty cycle of the boost using MPPT algorithm, generating PWM signals for the inverter, controlling other switches and relays in the circuit and determining the mode of operation of the circuit. To carry out these processes and functions, the hardware needs a brain. A dsPIC33FJ64MC802 has the capability of handling all these processes.

This dsPIC is 16 bit digital signal controller with motor control PWM and advanced analog conversion. It has 28 pins, out of which 21 pins are I/O pins. This dsPIC requires a voltage supply between 3 V and 3.6 V, which is provided by LM317. It has 2 PWM registers, one of them having the capability of generating 3 PWMs, that is 6 PWM signals. These are sent to the inverter. The second register has been used to generate the duty cycle for the boost converter. Thus, it has in all 8 PWM pins. Other I/O pins have a multifunctional capabilities and they can be run as per the requirements. Here, three of them are used to sense the input voltage, output voltage and input current. Another pin is used as an output pin to turn switch connected to the dissipation resistance ON and OFF.

The signals sent out from the dsPIC will only have a voltage level of 3V. Since the MOSFETS and relay need a higher voltage to turn ON, a non-inverting driver has been used. These drivers are MIC4422ZT. The signals coming from the dsPIC are sent to the input of the drivers. VCC of the drivers are connected to the output of LM7815, which makes VCC 15 V. Thus, when signal at the input of the driver is 3 V, it gives an output signal of 15 V and when the input to the driver is 0 V, the drivers output is 0 V. The PWM signals sent to the inverter do not need the drivers, the inverter can work with 3 V signals. However, the MOSFETS and relay need higher voltage. As a result, three drivers have been used for the same.

5. EXPERIMENTAL RESULTS

5.1 Introduction

The hardware was set up as described in chapter 3. Since it was not possible to capture results when connected with the solar panels, pictorial results were gathered with voltage sources by keeping the duty cycle of the boost converter constant. Results were also gathered with the PV panels as the input, however those were noted down using a multimeter.

To give input without the solar panels, two variable DC sources were used. One of them was connected to VIN1. This DC source was kept constant at 26 V. This was supplying voltage for the voltage regulators. The other DC source was connected to VIN2. Voltage applied through this DC source was varied continuously so as to obtain results. This chapter discusses the results obtained from this setup and also the setup with panels.

5.2 Results with DC sources

When two variable DC sources were used as explained above, only one thing needed to be done to run it. It was adjusting the duty cycle of the boost converter. This is because if there were PV panels, the MPPT algorithms would define that duty cycle. However with the variable DC sources, the MPPT algorithm would not work. Hence the duty cycle needs to be defined prior to the operation of the motor.

One observation about the mode of operation of the boost converter was that when the motor control switch was ON, the inverter was receiving PWM signals from the dsPIC and the motor was connected to the circuit. The boost converter was operating in continuous conduction mode irrespective of the duty cycle set for the

boost converter. However when that switch was OFF, the inverter gets open circuited isolating the motor from the circuit. A high value resistance is then connected as a load in this mode of operation. As a result of this, the value of the current drops and the boost converter goes into discontinuous mode of operation. This causes the output voltage of the boost converter to be tripled or quadrupled even for a duty cycle of 0.5 when the input voltage should ideally be doubled as per equation 4.1. To avoid this high voltage, the duty cycle of the boost converter needs to be set to 0.1 so the voltage level across the output does not go beyond control.

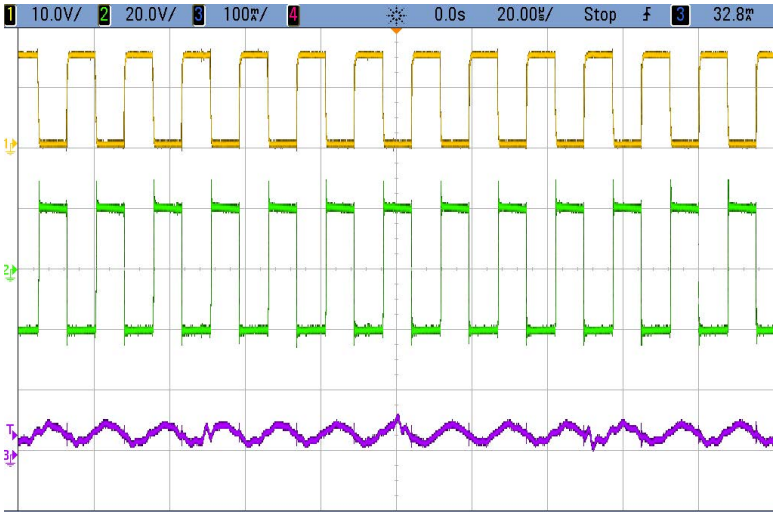

Fig. 5.1. Continunous conduction mode operation.

Fig. 5.1 shows the waveforms collected when the motor control switch is ON. Plot 1 (yellow) is the gating signal to the switch in the boost converter. Plot (green) is the voltage across the boost inductor. Plot 3 (purple) is the current flowing through the inductor. During this operation, the duty cycle is set as 0.5, which can be seen from plot 1 in Fig. 5.1. The voltage across the inductor (green) keeps fluctuating between +20 V and -20 V due to its charging and discharging. Plot 3 (purple) shows the inductor current. This current never goes to 0, thus operating the boost converter in continuous conduction mode. At this point the output voltage will be a direct function of the input voltage as per equation 4.1.

Operation of the boost converter is shown in the Fig. 5.2. Plot 1(yellow) is the gating signal to the switch in the boost converter. Plot 2 (green) is the voltage across the boost inductor. Plot 3 (purple) is the current flowing through the inductor. When the motor control switch is OFF, the PWM signals sent to the inverter are such that the three switches on the top of each leg of the inverter are ON and the three switches on the bottom of the three legs are OFF. Also the dissipation resistance is connected in the circuit. The high value of this resistance restricts the current flowing through the circuit to a very low value, thus operating the boost converter in discontinuous mode. If the duty cycle is kept at 0.5, the output voltage is almost four times the input voltage, which is dangerous for the capacitors connected across the DC link voltage of the inverter. To reduce this voltage, duty cycle of 0.1 is set for boost converter switch. The voltage only doubles at the most with this duty cycle.

This same problem can also occur when the PV panels are used instead of a DC source. Hence the same procedure is followed after the motor control switch is turned OFF. The duty cycle for the boost is not decided by MPPT algorithm anymore then and is set constant at 0.1.

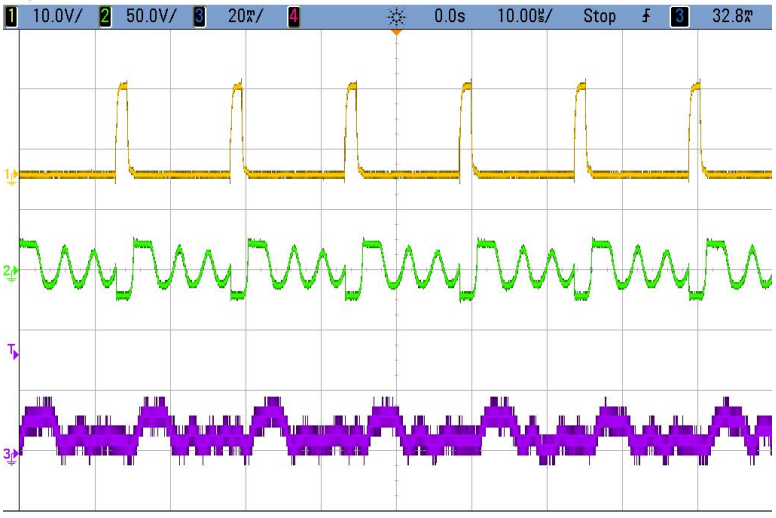

Fig. 5.2. Discontinunous conduction mode operation.

5.2.1 Motor starting

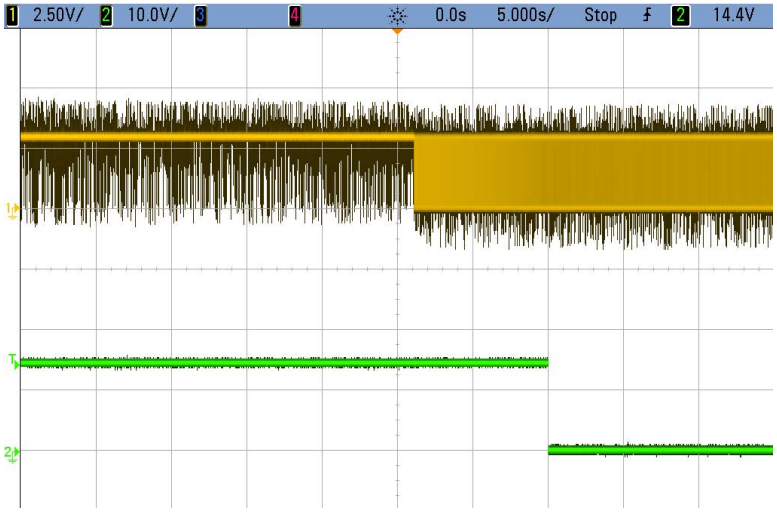

Fig. 5.3. Starting procedure of the motor.

The starting current for the motor goes up to six to seven times the steady state current. A current of this high magnitude, even for a short time can be potentially damaging to the components in the circuit. To curtail this current, a start-up procedure has been adopted which has been explained in detail in chapter 3.

As per this procedure, when the motor control switch is OFF, the switch connected in series with the dissipation resistance must be ON. Also, the inverter must get constant high signals of three switches. When the motor control switch is turned ON, the modulation index is gradually increased to 1, thus slowly increasing the voltage applied to the motor. Only when the modulation index reaches 1, the dissipation resistance should be disconnected from the circuit. The ramp for modulation index increase was designed for 10 seconds to guarantee a very low starting current. It can be seen from Fig. 5.3 that the dissipation resistance was connected for 10 seconds, until the modulation index increased to 1 and then the switch turned off, disconnecting the dissipation resistance from the circuit.

The start-up current can be seen in Fig. 5.4. Plot 1 (yellow) is the output voltage of the boost converter. Plot 2 (green) is the input given to the boost converter. Plot

3 (purple) is the current drawn from the DC source. When the motor control switch is turned ON, there is a sharp increase in the current drawn from the source. This is starting current is very low as compared to what it is without this start-up procedure. There is also a small temporary drop in the voltage drawn from the DC source and subsequently the output of the boost as well, however it reaches a steady value once the starting current settles.

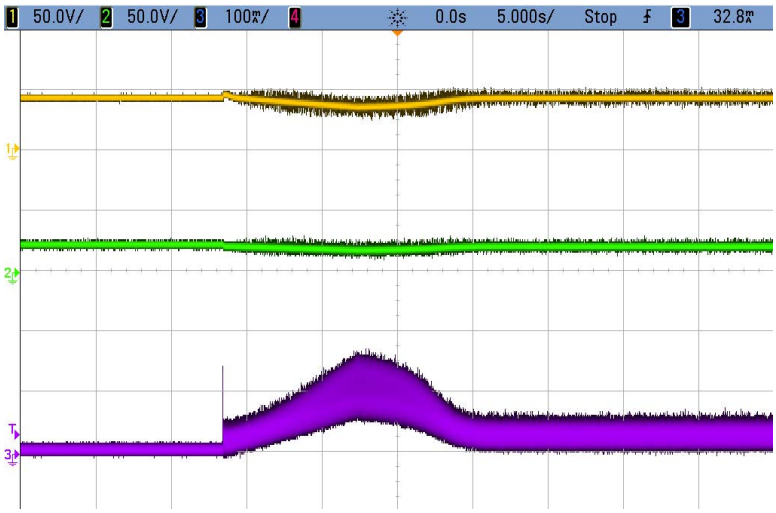

Fig. 5.4. Starting procedure of the motor.

5.2.2 Motor Stopping

When the motor control switch is turned OFF, the inverter should not suddenly received constant PWM signals for its switches which would isolate the motor from the circuit. This would cause an abrupt stopping for the motor. It would also suddenly drop the current in the boost converter circuit. This needs to be avoided. For this purpose, a stopping procedure was developed and explained in chapter. It is similar to the start-up procedure, but in the reverse order. When the motor control switch is turned OFF, the signal to the switch connected in series with the dissipation

resistance must go high. Instead of abruptly shorting the inverter, the modulation index for the PWM signals must be decreased from 1 to 0 and then the PWM signals sent should be a constant high or constant low, isolating the motor from the circuit.

A ramp equation was designed to reduce the modulation index for the PWM from 1 to 0 in 10 seconds, after which the motor should be isolated from the circuit. This can be seen from Fig. 5.5. Plot 1 (yellow) is the PWM signals sent to one of the switches. Plot 2 (green) is for the gating signal for the switch connected in series with dissipation resistance. When the motor control switch is turned OFF, the gating signals for the dissipation resistance switch go high, but PWM signals are still being generated on a constantly reducing modulation index. When the modulation index becomes 0 after 10 seconds, the PWM signals become either a constant high or a constant low, isolating the motor from the circuit.

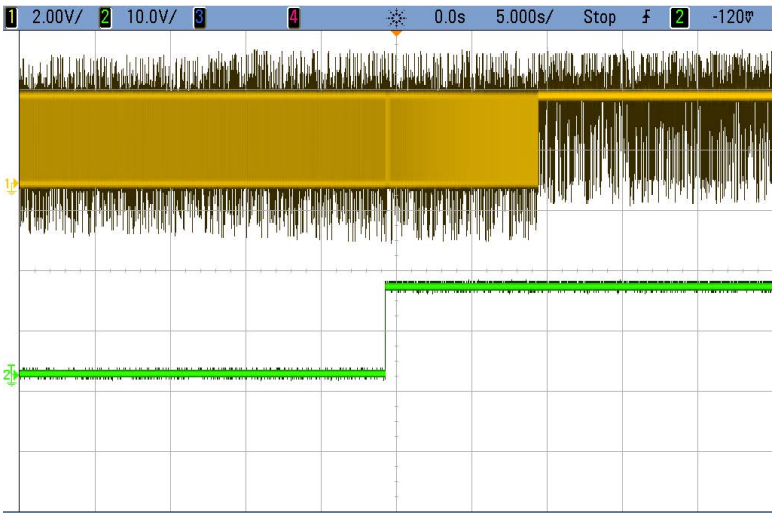

Fig. 5.5. Starting procedure of the motor.

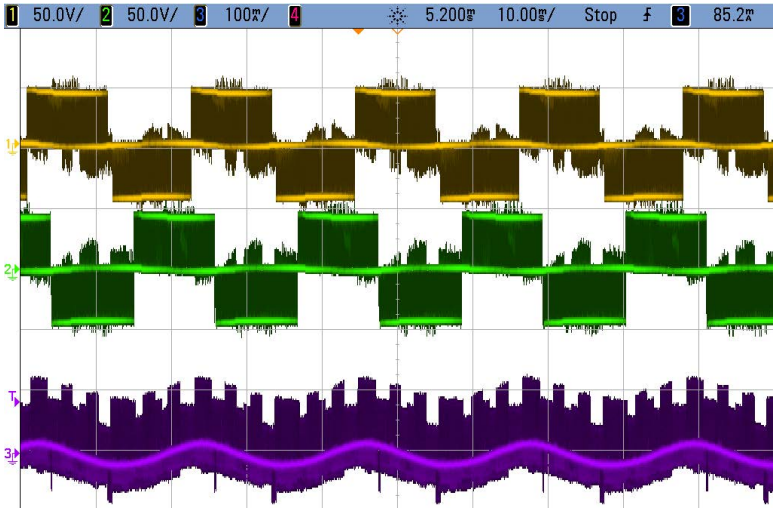

Fig. 5.6. Output voltages and current.

5.2.3 Output voltages and currents

The plots for AC output voltages across the motor can be seen in the first two plots of Fig. 5.6. It shows a line to line voltage with 3 levels. Phase to ground voltage is however a 5 level voltage. The third plot in Fig. 5.6 shows the current flowing through one of the phases. Thus the AC motor was run successfully using a DC source to get the above results.

5.3 Results with PV panels

6 PV panels were connected in series as described in chapter 4. Fig. 5.7 shows the panels being connected in series for the experiment.

Connections of 6 panels in series gave a total input voltage of 126 V. The magnitude of the signal sent to the gate of the switch of the boost converter is 15 V. With the test done previously with a DC source, voltage applied to the gate of that switch shows approximately 7.5 V when a 50% duty cycle is applied to the switch. This basically shows the average value of the signal applied. Now when this test with PV panels was done, the voltage applied to the switch of the boost converter was

Fig. 5.7. Panel connection.

seen to be fluctuating between 1.7 V and 3.1 V, which implies that the duty cycle was varying between 11% and 21%, ensuring maximum power point operation. The output of the boost converter was seen to be around 150 V.

The results gathered show that the system can work effectively to run the motor with MPPT, Volts Hertz for below rated voltage conditions and modulation index compensation methods for voltages higher than the rated values of the motor.

6. CONCLUSION

The motor was successfully operated incorporating MPPT, Volts-Hertz and modulation index compensation method such that the motor is always run at its optimal condition. MPPT ensured that maximum power was always being extracted from the PV panels. The Perturb and Observe method was used for maximum power point tracking. To implement it, a boost converter was used, whose duty cycle was defined by the MPPT algorithm. Operating the motor directly at a voltage lower than its rated voltage would not give maximum torque per ampere. As a result, Volts-Hertz method was implemented to adjust the frequency of operation of the motor as per the voltage available for its operation. This method keeps the flux of the motor at its rated value, certifying maximum torque per ampere operation. For voltage higher than the rated value, operation of the motor needs to be done carefully. This is because the motor tends to saturate if the voltage increases too much, thus drawing more current to magnetize the circuit. To avoid this from happening, modulation index compensation was used. Although the instantaneous voltage applied to the voltage reaches a high value, the RMS value of the voltage applied to the motor can be kept constant by adjusting the modulation index of the carriers defining the PWM signals for the inverter. As the voltage increases above the rated value, modulation index decreases from 1 depending upon the input voltage level to keep the RMS value of the motor at its rated value.

Even though all the above processes worked well initially, there still was a problem with respect to turning the motor ON and OFF irrespective of the presence of input voltage. This problem was sorted by using a motor control switch which could turn the motor ON and OFF whenever needed. Another issue which had to be tackled once this switch was added was to control the current drawn from the source. A sudden high current is never good for any circuit or its components. To solve it, an

algorithm explained in chapter 3 was designed to start and stop the motor smoothly and avoiding any damage to the components in the circuit. To start the motor, modulation index was increased from 0.1 to 1 over a period of 10 seconds so the voltage applied gradually increases, which is the concept used in soft starting of a motor. The starting current drawn source was subsidised immensely using this algorithm. A similar method was used for stopping the motor, just that the modulation index was decreased from 1 to 0, thus slowly reducing the voltage applied to the motor before eventually turning it off. The dissipation resistance plays a very important in this design for starting and stopping.

This implementation was done for a conventional inverter which gives a 5 level phase to ground output voltage. The quality of the waveform is not as good as the proposed topology in chapter three. The number of levels can be increased to twice its present value by adding a flyback converter to the conventional inverter as a part of cascaded operation. As inferred in chapter 3, it also proves that the quality of the waveforms in terms of the THD is much better for the proposed circuit. The future extension of this project can be adding the flyback converter to get a better quality output voltage, operating the motor with better AC voltage.

REFERENCES

REFERENCES

[1] Cs. Szab, I. I. Incze and M. Imecs. "Voltage-Hertz Control of the Synchronous Machine with Variable Excitation," *2006 IEEE International Conference on Automation, Quality and Testing*, vol. 1, pp. 298-303, May 2006.

[2] W. Hoffinann, "PV Solar Electricity: One Among The New Millennium Industries," *17th European Photovoltaic Solar Energy and Conference and exhibition, Munich, Germany*, pp. 22-26, October 2001.

[3] F. Jiang and A. Wong, "Study on the Performance of Different Types of PV Modules in Singapore," *The 7th International Power Engineering Conference, 2005*, pp. 1-109, November-December 2005.

[4] M. M. Ahmed and M. Sulaiman, "Design and Proper Sizing of Solar Energy Schemes for Electricity Production in Malaysia," *PECon 2003 Proceedings National Power Engineering Conference, 2003*, pp. 268-271, December 2003.

[5] P. K. Steimer, Enabled by High Power Electronics - Energy efficiency, Renewables and Smart Grids, *The 2010 International Power Electronics Conference*, pp. 11-15, 2010.

[6] E. dos Santos, C. B. Jacobina, E. da Silva and Nady Rocha, "Single-Phase to Three-Phase Power Converters: State of the Art," *IEEE Transactions on Power Electronics*, vol. 27, no. 5, pp. 2437-2452, May 2012.

[7] Q. Zhao and F. C. Lee, "High-Efficiency, High Step-Up DCDC Converters," *IEEE Transactions on Power Electronics*, vol. 18, no. 1, pp. 65-73, January 2003.

[8] L. M. Tolbert, F. Z. Peng and T. G. Habetler, "Multilevel converters for large electric drives," *IEEE Transactions on Industry Applications*, vol. 35, no. 1, pp. 36-44, January-February 1999.

[9] J. S. Lai and F. Z. Peng, "Multilevel converters A new breed of power converters," *IEEE Transactions on Industry Applications*, vol. 32, no.3, pp. 509-517, May-June 1996.

[10] J. Rodrguez, J. Lai and F. Peng, "Multilevel inverters: a survey of topologies, controls and applications," *IEEE Transactions on Industry Applications*, vol. 49, no. 4, pp. 724-738, August 2002.

[11] Z. Du, L. M. Tolbert and J. N. Chiasson, "A Cascade Multilevel Inverter Using a Single DC Source," *IEEE Applied Power Electronics Conference, Dallas, Texas*, pp. 426-430, March 2006.

[12] K.A. Corzine, F.A. Hardrick and Y.L. Familiant, "A Cascaded Multilevel H-Bridge Inverter Utilizing Capacitor Voltages Sources," *Proceedings of the IASTED Internatinal Conference, Power and Energy Systems, Palm Springs, California*, pp. 290-295, February 2003.

[13] Z. Du, B. Ozpineci, L. M. Tolbert and J. N. Chiasson, "Inductorless DC-AC Cascaded H-bridge Multilevel Boost Inverter for Electric/Hybrid Electric Vehicle Applications," *Industry Applications Conference, 2007*, pp. 603-608, September 2007.

[14] A.F. Okou, O. Akhrif , R. Beguenane and M. Tarbouchi, "Nonlinear control strategy insuring contribution of PV generator to voltage and frequency regulation," *6th IET International Conference on Power Electronics, Machines and Drives*, pp. 1-5, March 2012.

[15] L. D. Watson and J. W. Kimball. "Frequency regulation of a microgrid using solar power," *26th Annual IEEE, Applied Power Electronics Conference and Exposition (APEC)*, pp.321-326, March 2011.

[16] J. A. P. Lopes, C. L. Moreira and A. G. Madureira, "Defining control strategies for microgrids islanded operation," *IEEE Transactions on Power System*, vol. 21, no. 2, pp. 439-449, May 2006.

[17] C. Wang and M. H. Nehrir, "Power management of a stand-alone wind/photovoltaic/fuel cell energy system," *IEEE Transactions on Energy Conversion*, vol. 23, no. 3, pp. 957-967, September 2008.

[18] B. Belvedere, M. Bianchi, A. Borghetti, C. A. Nucci, M. Paolone and A. Peretto, "A microcontroller-based power management system for standalone microgrids with hybrid power supply," *IEEE Transactions on Sustainable Energy*, vol. 3, no. 3, pp. 422-431, July 2012.

[19] K. T. Tan, X. Y. Peng, P. L. So, Y. C. Chu and M. Z. Q. Chen, "Centralized control for parallel operation of distributed generation inverters in microgrids," *IEEE Transactions on Smart Grid*, vol. 3, no. 4, pp. 1977-1987, December 2012.

[20] B. Wang, M. Sechilariu and F. Locment, "Intelligent DC microgrid with smart grid communications: Control strategy consideration and design," *IEEE Transactions on Smart Grid*, vol. 3, no. 4, pp. 2148-2156, December 2012.

[21] K. T. Tan, P. L. So, Y. C. Chu and M. Z. Q. Chen, "Coordinated control and energy management of distributed generation inverters in a microgrid," *IEEE Transactions on Power Delivery*, vol. 28, no. 2, pp. 704-713, April 2013.

[22] J. Kim, J. Jeon, S. Kim, C. Cho, J. Park, H. Kim and K. Nam, "Cooperative control strategy of energy storage system and microsources for stabilizing the microgrid during islanded operation," *IEEE Transactions on Power Electronics*, vol. 25, no. 12, pp. 3037-3048, December 2010.

[23] T. Dragicevic, J. M. Guerrero J. C. Vasquez, and D. Skrlec, "Supervisory control of an adaptive-droop regulated DC microgrid with battery management capability," *IEEE Transactions on Power Electronics*, vol. 29, no. 2, pp. 695-706, February 2014.

[24] W. A. Omran, M. Kazerani and M. M. A. Salama, "Investigation of methods for reduction of power fluctuations generated from large gridconnected photovoltaic systems," *IEEE Transactions on Energy Conversion*, vol. 26, no. 1, pp. 318-327, March 2011.

[25] H. Beltran, E. Bilbao, E. Belenguer, I. Etxeberria-Otadui and P. Rodriguez, "Evaluation of storage energy requirements for constant production in PV power plants," *IEEE Transactions on Industrial Electronics*, vol. 60, no. 3, pp. 1225-1234, March 2013.

[26] S. Teleke, M. E. Baran, S. Bhattacharya and A. Q. Huang, "Rule-based control of battery energy storage for dispatching intermittent renewable sources," *IEEE Transactions on Sustainable Energy*, vol. 1, no. 3, pp. 117-124, October 2010.

[27] S. Kim, J. Jeon, C. Cho, J. Ahn and S. Kwon, "Dynamic modeling and control of a grid-connected hybrid generation system with versatile power transfer," *IEEE Transactions on Industrial Electronics*, vol. 55, no. 4, pp. 1677-1688, April 2008.

[28] H. Fakham, D. Lu and B. Francois, "Power control design of a battery charger in a hybrid active PV generator for load-following applications," *IEEE Transactions on Industrial Electronics*, vol. 58, no. 1, pp. 85-94, January 2011.

[29] C. T. Rodrguez, D. V. de la Fuente, G. Garcera, E. Figueres and J. A. G. Moreno, "Reconfigurable control scheme for a PV microinverter working in both grid-connected and island modes," *IEEE Transactions on Industrial Electronics*, vol. 60, no. 4, pp. 1582-1595, April 2013.

[30] B. I. Rani, G. S. Ilango and C. Nagamani, "Control strategy for power flow management in a PV system supplying DC loads," *IEEE Transactions on Industrial Electronics*, vol. 60, no. 8, pp. 3185-3194, August 2013.

[31] J. Vieira and A. Mota, "Maximum Power Point Tracker Applied in Batteries Charging with PV Panels," *IEEE International Symposium on Industrial Electronics, 2008*, pp. 202-207, July 2008.

[32] M. A. G. de Brito, L. P. Sampaio, G. Luigi, G. A. e Melo and C. A. Canesin, "Comparative Analysis of MPPT Techniques for PV Applications," *2011 International Conference on Clean Electrical Power, 2011*, pp. 99-104, June 2011.

[33] M. A. G. de Brito, G. Luigi, L. P. Sampaio, G. de Azevedo e Melo and C. A. Canesin, "Evaluation of the Main MPPT Techniques for Photovoltaic Applications," *International Transactions on Industrial Electronics*, vol. 60, no. 3, pp. 1156-1167, October 2012.

[34] S. Haghbin, K. Khan, S. Zhao, M. Alakula, S. Lundmark and O. Carlson, "An Integrated 20-kW Motor Drive and Isolated Battery Charger for Plug-In Vehicles," *IEEE Transactions on Power Electronics*, vol. 28, no. 8, pp. 4013-4029, January 2013.

[35] M.C. Duffy, "Three-phase motor in railway traction", *IEEE Proceedings-A, Science, Measurement and Technology*, vol. 139, no. 6, pp. 329-337, November 1992.

[36] X. Wen, W. Hu, T. Fan and J. Liu, "Lifetime Model Research of Motor Drive System for Electric Vehicles," *Proceeding of International Conference on Electrical Machines and Systems, Seoul, Korea*, pp. 129-132, October 2007.

[37] J. S. Moghani and M. Heidari, "High Efficient Low Cost Induction Motor Drive for Residential Applications," *International Symposium on Power Electronics, Electrical Drives, Automation and Motion*, pp. 1399-1402, May 2006.

[38] X. Wand, C. Gan, Y. Hu, W. Cao and X. Chen, "Renewable Energy-fed Switched Reluctance Motor for PV Pump Applications," *IEEE Transportation Electrification Conference and Expo*, pp. 1-6, August-September 2014.

[39] R. Chinthamalla, K. S. Ganesh and S. Jain, "An optimal and Efficient PV System using two 2-level Cascaded 3-level inverter for Centrifugal Pump," *IEEE International Conference on Power Electronics, Drives and Energy Systems (PEDES)*, pp. 1-6, December 2014.

[40] J. C. Salmon, "A variable SPEED drive circuit topology for feeding a 3-phase inverter bridge with a combined current and voltage dc link," *5th European Conference on Power Electronics and Applications*, vol. 5, pp. 139-144, September 1993.

[41] H. B. Ertan and Y. Sener, "Sinus Output 3-Phase Inverter Topology for Improved Drive Efficiency," *16th International Power Electronics and Motion Control Conference and Exposition*, pp. 1350-1357, September 2014.

[42] H. Liu, L. M. Tolbert, S. Khomfoi, B. Ozpineci and Z. Du, "Hybrid Cascaded Multilevel Inverter with PWM Control Method," *IEEE Power Electronics Specialists Conference*, pp. 162-166, June 2008.

[43] S. N. Rao, D.V. A. Kumar and C. S. Babu, "New Multilevel Inverter Topology with reduced number of Switches using Advanced Modulation Strategies," *International Conference on Power, Energy and Control*, pp. 693-699, February 2013.

[44] E. Shivakumar, V. Somasekhar, K. K. Mohapatra, K. Copakumar, L. Umanand and S. K. Sinha, "A multi level space phasor based PWM strategy for an open - end winding induction motor drive using two inverters with different DC link voltages," *4th IEEE International Conference on Power Electronics and Drive Systems*, vol. 1, pp. 169-175, October 2001.

[45] B. Vafakhah, J. Salmon and A. M. Knight, "Interleaved Discontinuous Space-Vector PWM for A Multi-Level PWM VSI using a 3-phase Split-Wound Coupled Inductor," *IEEE Energy Conversion Congress and Exposition*, pp. 2912-2919, September 2009.

[46] P. Shrawane, "Induction Motor Open- and Closed-loop Control Using Volt-per-Hertz Controller," *12th International Power Electronics Congress*, pp. 97-101, August 2010.

[47] J. Moris, A. Navarro, J. Cuartas and B. Mohammed, "Multipurpose controlled three-phase inverter for motor driving and grid power injection applications," *International Conference on New Concepts in Smart Cities: Fostering Public and Private Alliances*, pp. 1-7, December 2013.

[48] M. A. G. de Brito, G. Luigi, L. P. Sampaio, G. de Azevedo e Melo and C. A. Canesin, "Evaluation of the Main MPPT Techniques for Photovoltaic Applications," *International Transactions on Industrial Electronics*, vol. 60, no. 3, pp. 1156-1167, October 2012.

[49] M. A. G. de Brito, L. P. Sampaio, G. Luigi, G. A. e Melo and C. A. Canesin, "Comparative Analysis of MPPT Techniques for PV Applications," *2011 International Conference on Clean Electrical Power, 2011*, pp. 99-104, June 2011.

[50] F. Liu, Y. Kang, Y. Zhang and S. Duan, "Comparison of P and O and hill climbing MPPT methods for grid-connected PV converter," *3rd IEEE Conference on Industrial Electronics and Applications*, pp. 804-807, June 2008.

[51] I. V. Banu, R. Benuiga and M. Istrate, "Comparative Analysis of the Perturb-and-Observe and Incremental Conductance MPPT Methods," emphThe 8th Internation Symposium on Advanced Topics in Electrical Engineering, pp. 1-4, May 2013.

[52] N. Femia, G. Petrone, G. Spagnuolo and M. Vitelli, "Optimization of Perturb and Observe Maximum Power Point Tracking Method," *IEEE Transactions on Power Electronics*, vol. 20, no. 4, pp. 963-973, July 2005.

[53] A. Munoz-Garca, T. A. Lipo and D. W. Novotny, "A New Induction Motor V/f Control Method Capable of High-Performance Regulation at Low Speeds," *IEEE Transactions on Industry Applications*, vol. 34, no. 4, pp. 813-821, July-August 1998.

[54] I. I. Incze, C. Szabo and M. Imecs, "Voltage-Hertz Strategy for Synchronous Motor with Controlled Exciting Field," *11th Internation Conference on Intelligent Engineering Systems*, pp. 247-252, July 2007.

[55] R. A. Hamilton and G. R. Lezan, "Thyristor adjustable frequency power supplies for hot strip mill run-out tables," *IEEE Transactions on Industry and General Applications*, vol. IGA-3, no. 2, pp. 168-175, March-April 1967.

[56] W. Shepherd and J. Stanway, "An experimental closed-loop variable speed drive incorporating a thyristor driven induction motor," *IEEE Transactions on Industry and General Applications*, vol. IGA-3, no. 6, pp. 559-565, November-December 1967.

[57] W. Slabiak and L. Lawson, "Precise control of a three-phase squirrelcage induction motor using a practical cyclconverter," *IEEE Transactions on Industry and General Applications*, vol. IGA-2, no. 4, pp. 274-280, July-August 1966.

[58] M. A. Vitorino, M. B. de R. Correa, C. B. Jacobina and A. M. N. Lima, "An Effective Induction Motor Control for Photovoltaic Pumping," *IEEE Transactions On Industrial Electronics*, vol. 58, no. 4, pp. 1162-1170, April 2011.

[59] Y. Yao, P. Bustamante and R. S. Ramshaw, "Improvement of induction motor drive systems supplied by photovoltaic arrays with frequency control," *IEEE Transactions on Energy Conversion*, vol. 9, no. 2, pp. 256-262, June 1994.

[60] A. Barchowsky, J. P. Parvin, G. F. Reed, M. J. Korytowski and B. M. Grainger, "A Comparative Study of MPPT Methods for Distributed Photovoltaic Generation," *IEEE PES Innovative Smart Grid Technologies*, pp. 1-7, January 2012.

[61] M. F. Yaden, K. Kassmi, M. El Quariachi, B. Tidhaf, T. Mrabti, E. L. Chadli and K. Kassmi, "Design and Realization of a Photovoltaic System Equipped with a Digital MPPT Control," *International Conference on Multimedia Computing and Systems*, pp. 1-6, April 2011.

[62] Y. H. Wang, W. C. Liu and T. H. Kuo, "A 200W MPPT Boost Converter for BIPV Applications with Integrated Controller," *International Symposium on Computer, Consumer and Control*, pp. 288-291, June 2014.

[63] V. T. Somasekhar, B. V. Reddy and K. Sivakumar, "A Four-Level Inversion Scheme for a 6n-Pole Open-End Winding Induction Motor Drive for an Improved DC-Link Utilization," *IEEE Transactions on Industrial Electronics*, vol. 61, no. 9, pp. 4565-4572, September 2014.

[64] N. Femia, D. Granozio, G. Petrone, G. Spagnuolo and M. Vitelli, "Predictive Adaptive MPPT Perturb and Observe Method," *IEEE Transactions on Aerospace and Electronic Systems*, vol. 43, no. 3, pp. 934-950, July 2007.

[65] E. dos Santos Jr., J. H. G. Muniz, E. R. C. da Silva and C. B. Jacobina, "Nested Multilevel Topologies," *IEEE Transactions on Power Electronics*, vol. 30, no. 8, pp. 4058-4068, August 2015.

[66] N. Li, Y. Wang, W. Cong and Z. Wang, "Comparative Study of Four Kinds of Multicarrier PWM Strategies Used In NPC Three-Level Converters," *ECCE Asia Downunder*, pp. 183-189, June 2013.

[67] J. Larabee, B. Pellegrino and B. Flick, "Induction Motor Starting Methods and Issues," *Industry Applications Society 52nd Annual Petroleum and Chemical Industry Conference*, pp. 217-222, September 2005.

[68] B. A. Begum and J. A. Vasanth, "MPPT Based Photovoltaic Boost Half Bridge Converter for Grid Connected System," *International Conference on Green Computing Communication and Electrical Engineering*, pp. 1-6, March 2014.